StrucOpt manuscript No.
(will be inserted by the editor)

Detecting the stress fields in an optimal structure II: Three-dimensional case

A. Cherkaev and İ. Küçük

Abstract This paper is the second part of the investigation on stress fields in an optimal elastic structure. In the first part of this research, Cherkaev and Küçük (2001), we derived the necessary conditions for the stress field in optimal two-dimensional elastic structures and introduced a method to check if a structure is optimal. In this paper, we turn our attention to conditions of the stress field in optimal three-dimensional elastic structures. We restate the necessary conditions for minimization of the stress energy in three-dimensional elasticity. We also show that the conditions are realized in optimal microstructres.

1 Introduction

The structures for optimal three-dimensional elasticity were introduced and investigated in the papers: Gibiansky and Cherkaev (1987); Lipton and Diaz (1995); Cherkaev and Palais (1997); Allaire et al. (1997); Olhoff et al. (1998); Küçük (2001). The authors used the sufficient conditions (translation method) to compute the lower bound of the energy and demonstrated that the guessed structure correspond to this bound; this demonstration proved simultaneously the optimality of structures and bounds.

Here we investigate the fields inside of optimal structures using classical technique of the calculus of variations. The method of structural variation was introduced in books Lurie (1975, 1993); we use a version of it developed in a book Cherkaev (2000).

The stress fields within an optimally designed elastic structure satisfies certain conditions. These conditions show that the homogenized constitutive equations are on the boundary of ellipticity. Accordingly, the homogenized energy of an optimally designed elastic structure is on the boundary of quasiconvexity (see, for example, Cherkaev (2000)). Here, we derive and analyze the pointwise fields in optimal structures.

Most of the calculations are performed using MAPLE. If the derived formulas are too bulky, we do not display them, here; instead we refer to figures and the algorithm given in the Appendix. Detailed calculations can be found in Küçük (2001).

Received: August 24, 1998

A. Cherkaev and İ. Küçük

Department of Mathematics, University of Utah, Salt Lake City, Utah, USA
e-mail: `cherk@math.utah.edu` and e-mail: `kucuk@math.utah.edu`

2 Formulation of the Problem

Geometry Consider a domain Ω that is divided into two subdomains Ω_1 and Ω_2. Suppose that the subdomains Ω_i are occupied by isotropic materials with bulk and shear moduli of κ_i and μ_i, respectively. Suppose also that the volumes of Ω_1 and Ω_2 are fixed:

$$\int_\Omega \chi d\Omega = M_1$$

where $\chi(x)$ is the characteristic function defined as follows

$$\chi(x) = \begin{cases} 0 & \text{if } x \in \Omega_1, \\ 1 & \text{if } x \in \Omega_2. \end{cases} \tag{1}$$

Finally, assume that γ_1 and γ_2 are the cost of *Material 1* and *Material 2*, respectively.

Elasticity Consider the elastic equilibrium in the domain Ω, assuming the absence of body forces; a load is applied from the boundary Γ_T of Ω. A linearly elastic structure at equilibrium satisfies elasticity equations;

$$\nabla \cdot \boldsymbol{\sigma}(x) = 0, \qquad \boldsymbol{\epsilon} = \frac{1}{2}(\nabla u + (\nabla u)^T),$$
$$\boldsymbol{\epsilon}(x) = \boldsymbol{\mathcal{S}}(x)\boldsymbol{\sigma}(x), \tag{2}$$

where $\boldsymbol{\sigma}(x)$, and $\boldsymbol{\epsilon}(x)$ are three-by-three stress and strain tensors respectively, $\nabla = \left(\frac{\partial}{\partial x}, \frac{\partial}{\partial y}, \frac{\partial}{\partial z}\right)$ is the gradient, and $\boldsymbol{\mathcal{S}}(x)$ is the compliance tensor, carrying information about the material properties and associating two fields.

The energy of the elastic equilibrium is equal to

$$\boldsymbol{\mathcal{G}}(\chi, \boldsymbol{\sigma}) = \frac{1}{2}\boldsymbol{\sigma}(x) : \boldsymbol{\mathcal{S}}(x) : \boldsymbol{\sigma}(x); \tag{3}$$

second-rank stress tensors $\boldsymbol{\sigma}(x)$ belong to the set $\mathcal{F}^s(x)$ of statically admissible stress fields

$$\begin{aligned}\mathcal{F}^s(x) = \{\boldsymbol{\sigma}(x) \mid \nabla \cdot \boldsymbol{\sigma}(x) = 0 \; in \; \Omega, \\ \boldsymbol{\sigma}(x)\mathbf{n}(x) = \mathbf{t}(x) \; on \; \Gamma_T\}.\end{aligned} \tag{4}$$

Here, $\mathbf{t}(x)$ is given surface tractions; $\mathbf{n}(x)$ is the normal vector to the surface; and Γ_T is the surface where the traction is applied.

A fourth-rank material compliance tensor $\boldsymbol{\mathcal{S}}(x)$ belongs to the set of admissible compliance tensors, $\boldsymbol{\mathcal{S}}_{ad}$;

$$\boldsymbol{\mathcal{S}}(x) = \chi(x)\boldsymbol{\mathcal{S}}_1(\mu_1, \kappa_1) + (1 - \chi(x))\boldsymbol{\mathcal{S}}_2(\mu_2, \kappa_2), \tag{5}$$

μ_i and κ_i are shear and bulk moduli of the *i-th* material in the domain Ω.

The equilibrium of the structure corresponds to the principle of minimum of total stress energy; equations (2) are the Euler-Lagrange equation for the variational problem

$$\mathsf{E}(\chi) = \min_{\boldsymbol{\sigma}(x) \in \mathcal{F}^s(x)} \int_\Omega \boldsymbol{\mathcal{G}}(\chi, \boldsymbol{\sigma}) d\Omega, \tag{6}$$

where a solution $\boldsymbol{\sigma}(x)$ delivers the the minimum of the total stress energy (or maximum stiffness problem).

Optimal design Consider now a problem of optimal structure: Find $\chi(x)$ such that

$$\mathcal{J} = \min_{\chi(x)} \mathcal{W}(\chi); \quad \mathcal{W}(\chi) = [\mathsf{E}(\chi) + \gamma_1\chi + \gamma_2(1-\chi)], \tag{7}$$

It is expected that a solution to the optimization problem (7) includes fine-scale oscillations of the control $\boldsymbol{\mathcal{S}}(x)$ (see, for example, Cherkaev (2000)); in other words, the optimally designed structure is a *composite* or a limit of rapidly oscillating sequences of the original controls. The optimal distribution of the two materials can be described by a fastly oscillating sequence between the domains Ω_i. To deal with the fastly oscillating solutions, *relaxation* techniques are developed. The relaxation technique essentially replaces the original optimization problem with another one that has a classical solution.

Here we investigate the fields in the pure materials regardless of how wiggle is the line dividing the regions of them. Therefore, we do not use homogenization until final interpretation of results.

2.1 Notations for Calculations of Three-dimensional Elastic Composite

Calculations in a three-dimensional problem can be tedious unless appropriate notations are introduced. Therefore, the following basis is introduced to transform fourth- and second-rank tensors into six-by-six matrices or six-by-one vectors, respectably.

$$\begin{aligned}
&\mathbf{b}^{(1)} = \mathbf{i}_1 \otimes \mathbf{i}_1, \quad \mathbf{b}^{(5)} = \tfrac{1}{\sqrt{2}}(\mathbf{i}_1 \otimes \mathbf{i}_3 + \mathbf{i}_3 \otimes \mathbf{i}_1),\\
&\mathbf{b}^{(3)} = \mathbf{i}_3 \otimes \mathbf{i}_3, \quad \mathbf{b}^{(4)} = \tfrac{1}{\sqrt{2}}(\mathbf{i}_2 \otimes \mathbf{i}_3 + \mathbf{i}_3 \otimes \mathbf{i}_2),\\
&\mathbf{b}^{(2)} = \mathbf{i}_2 \otimes \mathbf{i}_2 \quad \mathbf{b}^{(6)} = \tfrac{1}{\sqrt{2}}(\mathbf{i}_1 \otimes \mathbf{i}_2 + \mathbf{i}_2 \otimes \mathbf{i}_1),
\end{aligned} \tag{8}$$

where

$$\mathbf{i}_1 = (1\ 0\ 0)^T, \quad \mathbf{i}_2 = (0\ 1\ 0)^T, \quad \text{and} \quad \mathbf{i}_3 = (0\ 0\ 1)^T. \tag{9}$$

are fixed reference Cartesian coordinates and dyadic product of two vectors, $\otimes$, is defined as

$$\begin{aligned}\mathbf{G} &= \mathbf{a} \otimes \mathbf{b},\\ &= \mathbf{a} \cdot \mathbf{b}^T \quad \text{or}\\ G_{ij} &= a_i b_j\end{aligned} \tag{10}$$

which is a second-rank tensor. Similarly, the dyadic product of m^{th}-rank tensor and k^{th}-rank tensor results in corresponding to $(m+k)^{th}$-rank tensor. The transformation rules

$$\mathcal{D}_{ij} = b^{(i)}_{\alpha\beta}\mathcal{S}_{\alpha\beta\kappa\eta}b^{(j)}_{\kappa\eta}, \quad i, j = 1, 2. \tag{11}$$

allow to express any stress tensor $\boldsymbol{\sigma}$ as a six-dimensional vector in the basis (8):

$$\boldsymbol{\sigma} = (\sigma_{11}\ \sigma_{22}\ \sigma_{33}\ \sqrt{2}\sigma_{12}\ \sqrt{2}\sigma_{13}\ \sqrt{2}\sigma_{23})^T. \tag{12}$$

Together with the notation (12), we shall use the following simpler notation in some calculations hereafter

$$\mathbf{s} = (s_1\ s_2\ s_3\ s_4\ s_5\ s_6)^T. \tag{13}$$

Similarly, any fourth-rank isotropic compliance tensor $\boldsymbol{\mathcal{S}}$ can be represented as six-by-six matrix

$$\boldsymbol{\mathcal{D}}_i = \begin{bmatrix} d_1 & d_2 & d_2 & 0 & 0 & 0\\ d_2 & d_1 & d_2 & 0 & 0 & 0\\ d_2 & d_2 & d_1 & 0 & 0 & 0\\ 0 & 0 & 0 & d_3 & 0 & 0\\ 0 & 0 & 0 & 0 & d_3 & 0\\ 0 & 0 & 0 & 0 & 0 & d_3 \end{bmatrix} \tag{14}$$

where

$$d_1 = \frac{1}{9}\frac{3\kappa_i + \mu_i}{\mu_i\kappa_i}, d_2 = -\frac{1}{18}\frac{3\kappa_i - 2\mu_i}{\mu_i\kappa_i}, \text{and } d_3 = \frac{1}{2\mu_i}.$$

The matrix $\boldsymbol{\mathcal{D}}_i$ is nondiagonal. Although we used a new notation $\boldsymbol{\mathcal{D}}$ for a transformed compliance tensor, $\boldsymbol{\mathcal{S}}$ will also be used for transformed compliance tensors hereafter in accordance with the usual convention.

3 Variations

3.1 The Scheme of the Weierstrass Test

A necessary condition of optimality, namely, the Weierstrass test is used to investigate the optimal design. This test deals with the increment of the functional caused by the special *structural variation*.

To perform the variation, we implant infinitesimal ellipsoidal inclusions filled with an admissible material $\boldsymbol{\mathcal{S}}_n$ at a proximity of a point x in the domain Ω_h that is occupied by a host material $\boldsymbol{\mathcal{S}}_h$. We compute the increment: The difference between the cost of the problem in two configurations with and without inclusion. If the examined structure is optimal, then the increment is nonnegative. The increment depends on the shape of the region of variation and must stay nonnegative for all inclusions; therefore the strongest condition corresponds to such a shape that the increment reaches its minimal value which must be also nonnegative. If this condition is violated, then the cost could be reduced by a variation, and the structure fails the test. The Weierstrass test was suggested in the described form by Lurie in the book Lurie (1975).

3.2 Variation of Properties: Three Dimensions

To calculate the variation of properties, add a quasiperiodic dilute composite of third-rank laminates to material $\boldsymbol{\mathcal{S}}_h$ in a neighborhood of the point x in accord with Cherkaev (2000). In these laminates, the inclusions are made of material $\boldsymbol{\mathcal{S}}_n$, and the envelope is made of material $\boldsymbol{\mathcal{S}}_h$. In other words, we construct a third-rank laminate from the isotropic host medium contained in the envelope. This matrix laminate composite of third-rank is characterized by its effective tensor $\boldsymbol{\mathcal{S}}_*$ given in Gibiansky and Cherkaev (1997a), (see also Francfort and Murat (1986) and Cherkaev (2000)) as

$$\boldsymbol{\mathcal{S}}_*(m) = \boldsymbol{\mathcal{S}}_h + m\left((\boldsymbol{\mathcal{S}}_n + \boldsymbol{\mathcal{S}}_h)^{-1} + (1-m)\boldsymbol{\mathcal{N}}^{3rd}(\boldsymbol{\alpha})\right)^{-1}, \tag{15}$$

where m is the volume fraction of the nuclei material; the matrix $\boldsymbol{\mathcal{S}}_i$ in the basis of (8) is given by (14); and matrix $\boldsymbol{\mathcal{N}}^{3rd}$ determines the geometry of the laminate:

$$\boldsymbol{\mathcal{N}}^{3th}(\boldsymbol{\alpha}) = \sum_{i=1}^{3}\alpha_i\boldsymbol{\mathcal{N}}_i, \quad \sum_{i=1}^{3}\alpha_i = 1, \quad \alpha_i \geq 0. \tag{16}$$

where

$$\boldsymbol{\mathcal{N}}_i = \mathbf{p}_i(\mathbf{p}_i^{\mathbf{T}}\boldsymbol{\mathcal{S}}_1\mathbf{p}_i)^{-1}\mathbf{p}_i^{\mathbf{T}}. \tag{17}$$

The matrix projector $\mathbf{p}_i$ maps the stress vector (4) into its discontinuous part; it depends on the normal $\mathbf{n}$ to the layers in the structure

$$\mathbf{p}_i = \mathbf{p}_i(\mathbf{n}). \tag{18}$$

Projection matrix $\mathbf{p}_i$ in $\boldsymbol{\mathcal{N}}_i$'s of (16) are given by (see Gibiansky and Cherkaev (1997a)):

$$\mathbf{p}_1 = \begin{bmatrix} 0&0&0\\1&0&0\\0&1&0\\0&0&0\\0&0&0\\0&0&1 \end{bmatrix}, \ \mathbf{p}_2 = \begin{bmatrix} 1&0&0\\0&0&0\\0&1&0\\0&0&0\\0&0&1\\0&0&0 \end{bmatrix}, \text{and } \mathbf{p}_3 = \begin{bmatrix} 1&0&0\\0&1&0\\0&0&0\\0&0&1\\0&0&0\\0&0&0 \end{bmatrix}. \tag{19}$$

In (19), the projection matrices point to the discontinuous components of stress fields in (4). The lamination directions $\mathbf{n}_k$ in the structure (18) are directed along $\mathbf{i}_k$.

Substituting (14), (16), and (19) into (15); and using the following notations for α's:

$$\alpha_1 = \alpha, \quad \alpha_2 = \beta \quad \text{and } \alpha_3 = 1-\alpha-\beta$$

in (15) result in

$$\boldsymbol{\mathcal{N}}^{3rd} = \begin{bmatrix} (1-\alpha)\mathfrak{e}_1 & \alpha_3\mathfrak{e}_2 & \beta\mathfrak{e}_2 & 0 & 0 & 0\\ \alpha_3\mathfrak{e}_2 & (1-\beta)\mathfrak{e}_1 & \alpha\mathfrak{e}_2 & 0&0&0\\ \beta\mathfrak{e}_2 & \alpha\mathfrak{e}_2 & (\alpha+\beta)\mathfrak{e}_1 & 0&0&0\\ 0&0&0&\alpha_3\mathfrak{e}_3&0&0\\ 0&0&0&0&\beta\mathfrak{e}_3&0\\ 0&0&0&0&0&\alpha\mathfrak{e}_3 \end{bmatrix}. \tag{20}$$

where $\alpha_3 = 1-(\alpha+\beta), \mathfrak{e}_1 = 4\frac{(3\kappa_h+\mu_h)\mu_h}{3\kappa_h+4\mu_h}$, $\mathfrak{e}_2 = 2\frac{(3\kappa_h-2\mu_h)\mu_h}{3\kappa_h+4\mu_h}$, and $\mathfrak{e}_3 = 2\mu_h$. The eigenvectors of $\boldsymbol{\mathcal{N}}^{3rd}$ are computed in the basis (8) that coincide with the directions of lamination in $\mathbb{R}^3$; the inner parameters α_i are responsible for relative elongation (intensities) of the inclusions.

Dilute inclusions The increment $\delta\boldsymbol{\mathcal{S}}$ caused by the array of infinitely dilute nuclei with material $\boldsymbol{\mathcal{S}}_n$ and infinitesimal volume fraction $\delta m(x)$ is given by

$$\delta m(x) = \begin{cases} \mathcal{O}(\epsilon), & \text{if } \|x-x_0\| < \epsilon,\\ 0, & \text{if } \|x-x_0\| \geq \epsilon. \end{cases} \quad \delta m \in C^1(\Omega), \tag{21}$$

similarly to the two-dimensional case. The effective property of this composite becomes $\boldsymbol{\mathcal{S}}_*(m+\delta m)$; it is calculated by Taylor's expansion;

$$\boldsymbol{\mathcal{S}}_*(m+\delta m) = \boldsymbol{\mathcal{S}}_*(m) + \delta m \frac{d}{dm}\boldsymbol{\mathcal{S}}_*(m) + \mathsf{o}(\delta m).$$

If we substitute the value of $\boldsymbol{\mathcal{S}}_*(m)$ from (15) into the last equation and compute

$$\lim_{m\to 0} \boldsymbol{\mathcal{S}}_*(m+\delta m) = \boldsymbol{\mathcal{S}}_h + \delta\boldsymbol{\mathcal{S}};$$

we obtain

$$\delta\boldsymbol{\mathcal{S}} = \mathbf{V}\delta m + \mathsf{o}(\delta m), \tag{22}$$

where

$$\mathbf{V} = \left((\boldsymbol{\mathcal{S}}_n - \boldsymbol{\mathcal{S}}_h)^{-1} + \boldsymbol{\mathcal{N}}^{3rd}(\boldsymbol{\alpha})\right)^{-1}. \tag{23}$$

Degeneration In contrast to the two-dimensional case, in three dimensions we meet several degenerative cases. Let us discuss them. The variation of (15) depends on two structural parameters α_1 and α_2 (or, in other notations, on α and β), such that

$$\alpha_1 \ge 0, \quad \alpha_2 \ge 0, \quad \alpha_1 + \alpha_2 \le 1.$$

If one of the α_i's is zero or if $\alpha_1 + \alpha_2 = 1$, the structure degenerates into a second-rank laminate with parallel cylindrical inclusions.

The effective tensor $\boldsymbol{\mathcal{S}}_*(m)$ of a second-rank laminate is similar to (15) and is given by the formula:

$$\boldsymbol{\mathcal{S}}_*(m) = \boldsymbol{\mathcal{S}}_h + m\left((\boldsymbol{\mathcal{S}}_n - \boldsymbol{\mathcal{S}}_h)^{-1} + (1-m)\boldsymbol{\mathcal{N}}_i^{2nd}(\boldsymbol{\alpha})\right)^{-1}, \tag{24}$$

where $\boldsymbol{\mathcal{N}}_i^{2nd}(\boldsymbol{\alpha})$ is

$$\boldsymbol{\mathcal{N}}_i^{2nd} = (\alpha_j - \delta_{ij}\alpha_i)\boldsymbol{\mathcal{N}}_j, \quad i,j = 1,2,3. \tag{25}$$

$\boldsymbol{\mathcal{N}}_j$ are defined in (17), and j is index of summation. Note that Einstein summation is used in (25), i.e., there is a summation on the repeated index j; δ_{ij} is the Dirak δ-function:

$$\delta_{ij} = \begin{cases} 1, & \text{if } i = j, \\ 0, & \text{if } i \ne j. \end{cases} \tag{26}$$

If both α_1 and α_2 are zero (or if one of them is equal to one), the structure degenerates into a first-rank laminate for which $\boldsymbol{\mathcal{N}}_i^{1st}(\boldsymbol{\alpha}) = \boldsymbol{\mathcal{N}}_3$.

Calculations of $\delta\boldsymbol{\mathcal{S}}$ these degenerative variations are performed similarly to (23), using $\boldsymbol{\mathcal{N}}^{2nd}$ computed in the expressions (25) or $\boldsymbol{\mathcal{N}}^{1st}$, respectively.

3.3 Increment

The increment of the functional consists of the *direct cost* caused by change of quantities of the used materials and the increment of energy. The first term is easy to compute: Replacing the host material $\boldsymbol{\mathcal{S}}_h$ (with the specific cost γ_n) with the material of $\boldsymbol{\mathcal{S}}_n$ (with the specific cost γ_h) leads to the change in the total cost.

Variation of energy Let us compute the variation of energy in (6) caused by the Weierstrass-type variation of properties $\delta\boldsymbol{\mathcal{S}}$. For simplicity, we consider such a variation that the axes of orthotropy of $\delta\boldsymbol{\mathcal{S}}$ are codirected with the principal axes of the stress tensor $\boldsymbol{\sigma}$ (the expression for $\delta\boldsymbol{\mathcal{S}}$ is given in (22)).

The increment of the energy δ_{E} is given by the quadratic form

$$\delta_{\mathsf{E}}(\alpha,\beta) = \mathbf{s}^{\mathbf{T}}\delta\boldsymbol{\mathcal{S}}(\alpha,\beta)\mathbf{s}, \tag{27}$$

and the total cost of the variation is

$$\Delta\mathcal{J}\delta m = (\gamma_h - \gamma_n + \delta_{\mathsf{E}}(\alpha,\beta))\,\delta m. \tag{28}$$

The increment (27) depends on the shape of the inclusions, specifically, on control parameters α and β (elongations) of the inclusions in the laminates. In the degenerative cases, the number of the parameters decreases.

Orientation of the inclusions As in two-dimensional case, we assume that the directions of laminates in the trial structure are codirected with the principal axes of the stress tensor. We codirect our labor coordinate system with the principle axes of the stress; this yields to

$$\mathsf{s}_4 = \mathsf{s}_5 = \mathsf{s}_6 = 0.$$

Substituting the expressions for $\mathbf{s}$ and $\delta\boldsymbol{\mathcal{S}}(\alpha,\beta)$ (see (13) and (23)) into (27) transforms the increment in the form:

$$\begin{aligned} \delta_{\mathsf{E}}(\alpha,\beta) &= \mathbf{s}^{\mathbf{T}}\delta\boldsymbol{\mathcal{S}}(\alpha,\beta)\mathbf{s}, \\ &= \mathbf{s}^{\mathbf{T}}\ \mathbf{V}\ \mathbf{s}\ \delta m, \\ &= \Big(\mathsf{V}_1\mathsf{s}_1^2 + \mathsf{V}_2\mathsf{s}_2^2 + \mathsf{V}_3\mathsf{s}_3^2 + 2\mathsf{V}_4\mathsf{s}_1\mathsf{s}_2 \\ &\qquad + 2\mathsf{V}_5\mathsf{s}_1\mathsf{s}_3 + 2\mathsf{V}_6\mathsf{s}_2\mathsf{s}_3\Big)\delta m. \end{aligned} \tag{29}$$

One can check that the coefficients V_i depend on controls α and β as follows:

$$\begin{aligned} \mathsf{V}_i = \frac{1}{\mathsf{K}}\Big(&\mathsf{V}_i^1(\kappa_h,\kappa_n,\mu_h,\mu_n)\alpha^2 + \mathsf{V}_i^2(\kappa_h,\kappa_n,\mu_h,\mu_n)\alpha\beta \\ &+ \mathsf{V}_i^3(\kappa_h,\kappa_n,\mu_h,\mu_n)\beta^2\Big) \end{aligned} \tag{30}$$

where K is a quadratic polynomial of α and β.

3.4 The Most Sensitive Variations

The analysis is similar to the two-dimensional case. If the design is optimal, then all variations lead to the non-negative increment $\delta\mathcal{J}$:

$$\delta\mathcal{J}(\boldsymbol{\mathcal{S}}_i, \boldsymbol{\mathcal{S}}_j, \boldsymbol{\sigma}_j) = \gamma_h - \gamma_n + \delta_{\mathsf{E}}(\alpha,\beta) \geq 0, \quad \forall\alpha,\beta \in \Xi \tag{31}$$

where $\delta\mathcal{J}(\boldsymbol{\mathcal{S}}_i, \boldsymbol{\mathcal{S}}_j, \boldsymbol{\sigma}_i)$ is a variation caused by adding material $\boldsymbol{\mathcal{S}}_j$ into material $\boldsymbol{\mathcal{S}}_i$, $\boldsymbol{\sigma}_i$ is the field in material $\boldsymbol{\mathcal{S}}_i$, and the set Ξ is

$$\Xi = \{\alpha, \beta \quad |0 \leq \alpha < 1, \quad 0 \leq \beta < 1 \text{ and } \alpha + \beta = 1\}. \tag{32}$$

If the condition (31) is violated, then the cost is reduced by the variation, and the design fails the test. Therefore, the optimal (most "dangerous") increment of energy (27) is

$$\mathbb{E} = \min_{\alpha,\beta\in\Xi} \delta_{\mathsf{E}}(\alpha,\beta). \tag{33}$$

If

$$\mathbb{E} > 0, \tag{34}$$

then the increment $\delta\mathcal{J} > 0$ for any variation and the structure satisfies the test.

3.4.1 Calculations of Optimal Parameters

Since the geometric shape of the variation is adjusted to the field $\boldsymbol{\sigma}$, we consider optimal parameters α and β as functions of $\boldsymbol{\sigma}$. Here we compute the derivative of $\delta\mathsf{E}(\alpha,\beta)$ given in (27), find optimal parameters, and calculate the optimal increment.

First we compute the derivative of the increment with respect to α and β in the form:

$$\begin{aligned} \frac{\partial\delta_{\mathsf{E}}(\alpha,\beta)}{\partial\alpha} &= \mathbf{s}^{\mathbf{T}}\frac{\partial\mathbf{V}(\alpha,\beta)}{\partial\alpha}\mathbf{s}, \\ &= -\mathbf{s}^{\mathbf{T}}\mathbf{V}(\alpha,\beta)\frac{\partial\mathbf{C}(\alpha,\beta)}{\partial\alpha}\mathbf{V}(\alpha,\beta)\mathbf{s}^{\mathbf{T}}, \end{aligned} \tag{35}$$

where $\mathbf{C}^{-1} = \mathbf{V}$; introduce a new variable $\boldsymbol{\nu}$:

$$\mathbf{V}(\alpha,\beta)\mathbf{s}^{\mathbf{T}} = \boldsymbol{\nu} \tag{36}$$

where $\boldsymbol{\nu} = (\nu_1\ \nu_2\ \nu_3\ \nu_4\ \nu_5\ \nu_6)$. Since the variables s_4, s_5 and s_6 are equal to zero, ν_4 ν_5 and ν_6 are zeros too, as it follows from (36). Therefore, we will not pursue the terms involving ν_4, ν_5, and ν_6 hereafter.

After substituting the new variable $\boldsymbol{\nu}$ into (35), we obtain

$$\frac{\partial\delta_{\mathsf{E}}(\alpha,\beta)}{\partial\alpha} = -\boldsymbol{\nu}^{\mathbf{T}}\frac{\partial\boldsymbol{\mathcal{N}}^{3rd}(\alpha,\beta)}{\partial\alpha}\boldsymbol{\nu}, \tag{37}$$

which amounts to the following quadratic equation for $\boldsymbol{\nu}$

$$\boldsymbol{\nu}^{\mathbf{T}}\ \frac{\partial\boldsymbol{\mathcal{N}}^{3rd}(\alpha,\beta)}{\partial\alpha}\ \boldsymbol{\nu} = 0. \tag{38}$$

Now we can repeat the same calculations for the derivative of $\delta\mathsf{E}(\alpha,\beta)$ with respect to β which amounts to the second quadratic equation:

$$\boldsymbol{\nu}^{\mathbf{T}}\ \frac{\partial\boldsymbol{\mathcal{N}}^{3rd}(\alpha,\beta)}{\partial\beta}\ \boldsymbol{\nu} = 0. \tag{39}$$

The next step is to solve the system of these equations (38) and (39) to determine the vector $\boldsymbol{\nu}$. Substituting this solution into (36) provides optimal values for α and β. We find that $\boldsymbol{\nu}$ belongs to one of the following sets;

$$\mathbb{V}_1 = \mathbb{V}_2 = \Big\{\boldsymbol{\nu}|\nu_1 = \nu_1, \nu_2 = \nu_3\Big\}, \tag{40}$$

and

$$\mathbb{V}_3 = \Big\{\boldsymbol{\nu}|\nu_1 = \mathfrak{U}, \nu_2 = \nu_2, \nu_3 = \nu_3\Big\}, \tag{41}$$

where

$$\mathfrak{U} = -\frac{1}{2}\frac{6\nu_2^2\kappa_h + 2\nu_2^2\mu_h - 6\nu_3^2\kappa_h - 2\nu_3^2\mu_h}{(\nu_2 - \nu_3)(3\kappa_h - 2\mu_h)}. \tag{42}$$

When one substitutes the vectors from $\mathbb{V}_1$ into (36), the optimal α's and β's are obtained as follows

$$\alpha_i = \frac{1}{6}\frac{\mathfrak{N}^{\alpha_i}}{\mathfrak{D}_i}, \qquad \beta_i = \frac{1}{6}\frac{\mathfrak{N}^{\beta_i}}{\mathfrak{D}_i}, \tag{43}$$

where $\mathfrak{N}^{\alpha_i}$, $\mathfrak{N}^{\beta_i}$, $\mathfrak{D}_i$ for $i = 1, 2$ are defined in Appendix A, and α and β are from the set Ξ given in (32).

Similarly, when vectors from set $\mathbb{V}_3$ are substituted into (36), the following optimal values of α's and β's are obtained

$$\alpha_j = \frac{1}{6}\frac{\mathfrak{N}^{\alpha_j}}{\mathfrak{D}_j}, \qquad \beta_j = \frac{1}{6}\frac{\mathfrak{N}^{\beta_j}}{\mathfrak{D}_j}, \tag{44}$$

where $\mathfrak{N}^{\alpha_j}$, $\mathfrak{N}^{\beta_j}$, $\mathfrak{D}_j$ for $j = 3, 4$ are defined in Appendix A, and α and β are from the set Ξ given in (32).

Degeneration If one of the parameters α_i or β_i computed in (43) and (44) is equal to zero or negative or if their sum is greater than one, then the optimal variation corresponds to a second-rank laminates. In this case, computation of the optimal variation $\delta\mathsf{E}(\alpha)$ follows from

(27) where (25) is used for the calculation of (23). Consequently, taking the first derivative of $\delta\mathsf{E}(\alpha)$ with respect to α gives the following minimizing values of α for different cases.

Case A: If $\alpha_3 = 0$, then $\alpha_1 = \alpha$, $\alpha_2 = 1-\alpha$ in (15). Thus, the optimal α is given by

$$\begin{aligned}\alpha_1^{2R3} &= \frac{1}{2}\frac{A_1\sigma_x + B_1\sigma_y + C_1\sigma_z}{D_1(\sigma_x+\sigma_y)+C_1\sigma_z},\\ \alpha_2^{2R3} &= \frac{B_2\sigma_x}{(\sigma_x-\sigma_y)} + \frac{C_2\sigma_y}{(\sigma_x-\sigma_y)} + \frac{A_2\sigma_z}{(\sigma_x-\sigma_y)}.\end{aligned} \tag{45}$$

Case B: If $\alpha_2 = 0$, then $\alpha_1 = \alpha$, $\alpha_3 = 1-\alpha$ in (15). Thus, the optimal α is given by

$$\begin{aligned}\alpha_1^{2R2} &= \frac{1}{2}\frac{A_1\sigma_x + C_1\sigma_y + B_1\sigma_z}{D_1(\sigma_x+\sigma_z)+C_1\sigma_y},\\ \alpha_2^{2R2} &= \frac{B_2\sigma_x}{(\sigma_x-\sigma_z)} + \frac{A_2\sigma_y}{(\sigma_x-\sigma_z)} + \frac{C_2\sigma_z}{(\sigma_x-\sigma_z)}.\end{aligned} \tag{46}$$

Case C: If $\alpha_3 = 0$, then $\alpha_2 = \alpha$, $\alpha_3 = 1-\alpha$ in (15). Thus, the optimal α is given by

$$\begin{aligned}\alpha_1^{2R1} &= \frac{1}{2}\frac{C_1\sigma_x + A_1\sigma_y + B_1\sigma_z}{C_1\sigma_x+D_1(\sigma_y+\sigma_z)},\\ \alpha_2^{2R1} &= \frac{A_2\sigma_x}{(\sigma_y-\sigma_z)} + \frac{B_2\sigma_y}{(\sigma_y-\sigma_z)} + \frac{C_2\sigma_z}{(\sigma_y-\sigma_z)},\end{aligned} \tag{47}$$

where

$$\begin{aligned}A_1 &= 3\kappa_h\kappa_n + 2\kappa_n\mu_h + 2\mu_n\kappa_h,\\ B_1 &= 2\kappa_n\mu_h - 3\kappa_n\kappa_h - 6\mu_h\kappa_h,\\ A_2 &= \frac{1}{3}\frac{(\mu_h+3\mu_n+3\kappa_h)(-\mu_n\kappa_h+\kappa_n\mu_h)}{\kappa_h(-\mu_h+\mu_n)(\mu_n-3\kappa_h-\mu_h+3\kappa_n)},\\ B_2 &= \frac{1}{6}\frac{B_3}{\kappa_h(-\mu_n+\mu_h)(-\mu_h+\mu_n-3\kappa_h+3\kappa_n)},\\ C_2 &= \frac{1}{6}\frac{C_3}{\kappa_h(\mu_n-\mu_h)(\mu_n-\mu_h-3\kappa_h+3\kappa_n)},\\ B_3 &= (-2\mu_h^2\kappa_n + (14\mu_n\kappa_h - 6\mu_n\kappa_n + 3\kappa_h\kappa_n)\mu_h\\ &\quad -3\mu_n\kappa_h(-2\kappa_h+2\mu_n+3\kappa_n))\\ C_3 &= (2(\kappa_n-3\kappa_h)\mu_h^2 + (6\mu_n\kappa_n + 15\kappa_h\kappa_n - 18\kappa_h^2\\ &\quad -2\mu_n\kappa_h)\mu_h - 3\mu_n\kappa_h(3\kappa_n-4\kappa_h))\\ C_1 &= 2(\kappa_n\mu_h - \mu_n\kappa_h),\\ D_1 &= (\mu_n\kappa_h - 3\mu_h\kappa_h + 2\kappa_n\mu_h).\end{aligned} \tag{48}$$

Here, α_i^{2Rj} denotes the optimal value of α_i when $\alpha_j = 0$ and the variation degenerates into a second-rank laminate. The energy increment is obtained by substitution of the optimal values α_i^{2Rj} into (27). The optimal variation becomes a first-rank laminate if two of the optimal values of α_i are zero or negative.

3.5 Necessary Conditions

The described condition (34) is satisfied in permit a region of fields in materials, and they are violated if the fields are outside of this permitted region. To describe the permitted regions we use the results of the Section 3.4.1. The range of admissible fields in an optimal structure is derived similarly to the two-dimensional case.

In this section, we consider a *well-ordered* case, $\mu_1 < \mu_2$ and $\kappa_1 < \kappa_2$. We fix the volume fraction of the first material $m_1 = m$ in the following calculations.

1. Suppose that a trial infinitesimal inclusion of the second (strong) material $\boldsymbol{\mathcal{S}}_2$ is placed into the domain Ω_1 occupied with the first (weak) material. The necessary condition $\delta\mathcal{J}(\boldsymbol{\mathcal{S}}_1, \boldsymbol{\mathcal{S}}_2, \boldsymbol{\sigma}_1)$ is obtained by formula (31) as
$$\delta\mathcal{J}(\boldsymbol{\mathcal{S}}_1, \boldsymbol{\mathcal{S}}_2, \boldsymbol{\sigma}_1) = \gamma_2 - \gamma_1 + \mathbb{E}(\boldsymbol{\mathcal{S}}_1, \boldsymbol{\mathcal{S}}_2, \boldsymbol{\sigma}_1) \geq 0, \tag{49}$$
where $\boldsymbol{\sigma}_1$ is the tested field in the domain Ω_1.
To calculate $\mathbb{E}(\boldsymbol{\mathcal{S}}_1, \boldsymbol{\mathcal{S}}_2, \boldsymbol{\sigma}_1)$, we use the algorithm given in Appendix (C). The inequality (49) depends only on the stress field $\boldsymbol{\sigma}_1$ since $\boldsymbol{\mathcal{S}}_1$ and $\boldsymbol{\mathcal{S}}_2$ are given. The set of fields $\boldsymbol{\sigma}_1$ that satisfies the condition (49) is called $\mathfrak{F}_1$. If $\boldsymbol{\sigma}_1 \in \mathfrak{F}_1$, then the weak material $\boldsymbol{\mathcal{S}}_1$ may be optimal in the sense that it cannot be denoted by the described variation. When the increment due to the inclusion of weak material into the strong material is calculated, the formula (23) is used where subscript $_h$ is 2.
2. Similarly we analyze the necessary condition of optimality of the (strong) material $\boldsymbol{\mathcal{S}}_2$. The corresponding increment $\delta\mathcal{J}(\boldsymbol{\mathcal{S}}_2, \boldsymbol{\mathcal{S}}_1, \boldsymbol{\sigma}_2)$ is due to the inserting of a trial inclusion of the first (weak) material $\boldsymbol{\mathcal{S}}_1$ into the domain Ω_2 occupied by the second (strong) material; the condition is given in (31).
$$\delta\mathcal{J}(\boldsymbol{\mathcal{S}}_2, \boldsymbol{\mathcal{S}}_1, \boldsymbol{\sigma}_2) = \gamma_1 - \gamma_2 + \mathbb{E}(\boldsymbol{\mathcal{S}}_2, \boldsymbol{\mathcal{S}}_1, \boldsymbol{\sigma}_2) \geq 0, \tag{50}$$
where $\boldsymbol{\sigma}_2$ is the field at a point of the domain Ω_2. To calculate $\mathbb{E}(\boldsymbol{\mathcal{S}}_2, \boldsymbol{\mathcal{S}}_1, \boldsymbol{\sigma}_2)$ we use the algorithm given in Appendix (C). The set of admissible fields $\boldsymbol{\sigma}_2$ that satisfies the condition (50) is called $\mathfrak{F}_2$. If $\boldsymbol{\sigma}_2 \in \mathfrak{F}_2$, then the strong material $\boldsymbol{\mathcal{S}}_2$ is optimal in the sense that it cannot be denoted by the described variation.

Remark 1 When the increment due to the inclusion of strong material into the weak material is calculated, the formula (23) becomes

$$\delta\boldsymbol{\mathcal{S}} = -\mathbf{V}\delta m + \mathsf{o}(\delta m), \quad \mathbf{V} = \left((\boldsymbol{\mathcal{S}}_2 - \boldsymbol{\mathcal{S}}_1)^{-1} + \boldsymbol{\Delta}\right)^{-1}$$

where subscript $_h$ in (23) is equal to one.

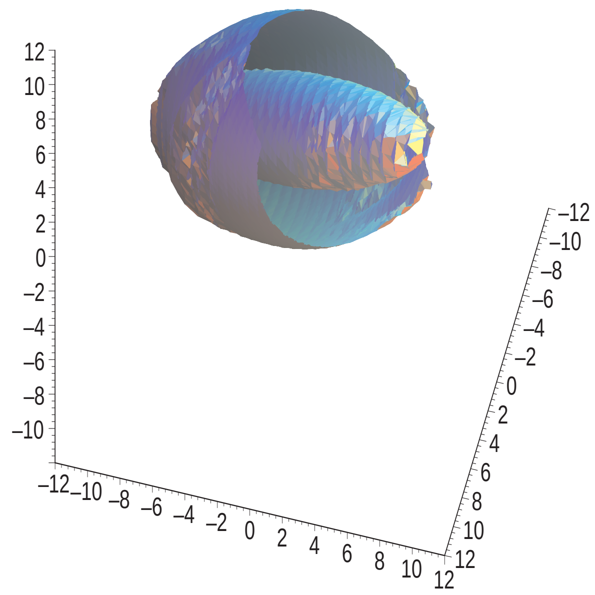

Fig. 1 Assembly of bounds: The interior region (intersection of ellipsoids) defines the bound of the set $\mathfrak{F}_1$ (stress in the weak material), the outer region defines the zone $\mathfrak{F}_2$ of optimality of the stress in the strong material, and the region between defines the forbidden region. One of the materials has zero Poisson ratio.

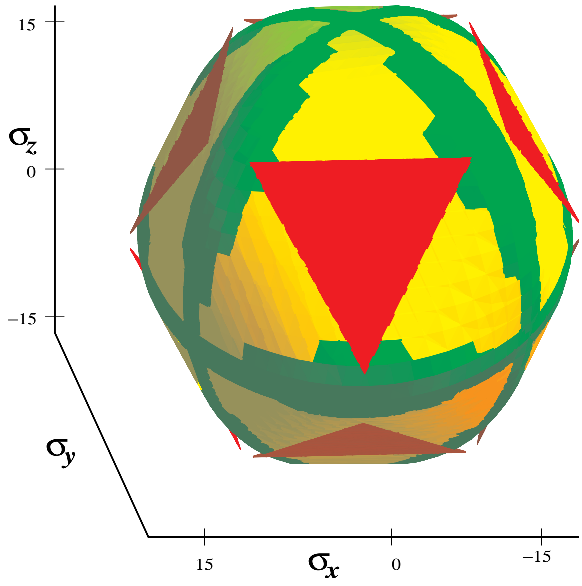

Fig. 2 The black triangular region is the third-rank laminate. White and gray regions show where the second and first-rank laminates are optimal, respectively. Both of the materials have nonzero Poisson ratio.

The union $\mathfrak{F} = \mathfrak{F}_1 \cup \mathfrak{F}_2$ of the two permitted sets does not coincide with the whole range of $\boldsymbol{\sigma}$. The remaining part is called the forbidden region, $\mathfrak{F}_f$. In this region, none of the materials is optimal. An optimal structure should be constructed in such a way that the local fields never belong to $\mathfrak{F}_f$, no matter what the external loading is.

The calculation of the set $\mathfrak{F}$ is based on the calculations of the sets $\mathfrak{F}_1$ and $\mathfrak{F}_2$ in each material $\boldsymbol{\mathcal{S}}_1$ and $\boldsymbol{\mathcal{S}}_2$ determined by (49) and (50), respectively.

4 Results

4.1 Range of Admissible Fields

The analysis above shows that the boundary of $\mathfrak{F}$ is an composition of three parts: An elliptical, cylindrical and plane part. The elliptical and the cylindrical parts respectively are given by the following expressions

$$\mathbb{E}_1 = A_3\sigma_i^2 + B_3(\sigma_j^2 + \sigma_k^2) = 1, \tag{51}$$

$$\mathbb{E}_2 = A_4\sigma_i^2 + B_4(|\sigma_j| + |\sigma_k|)^2 = 1, \tag{52}$$

where triplets i, j and k corresponds to some directions of x, y, z axes. The constants are determined by the materials' elastic properties; they correspond to optimal values of $\mathsf{E}(\alpha, \beta)$ at $\alpha = 0$, or $\alpha = 1$.

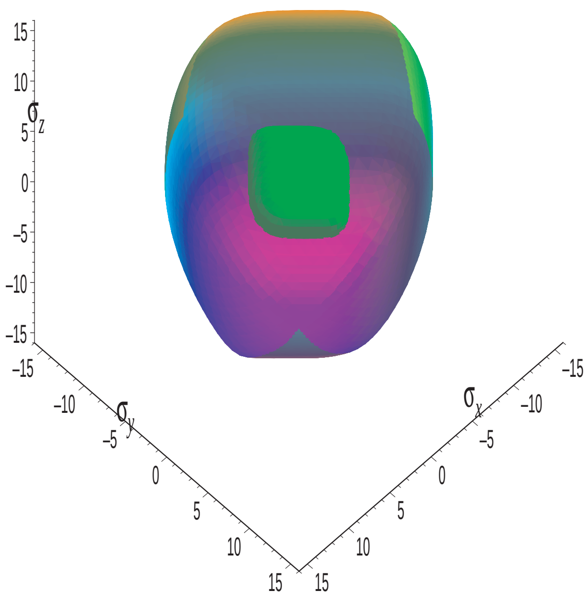

Fig. 3 The interior region of the small ellipsoid defines the bound of the set $\mathfrak{F}_1$, and the region between the ellipsoids defines the forbidden region when one of the materials has nonzero Poisson ratio.

Remark 2 The formula (52) shows the case when Poisson ratio of materials is zero. This formula is modified when the materials have an arbitrary Poisson ratio. In this case, the cylindrical and ellipsoidal parts are inclined on the angle defined by the Poisson ration.

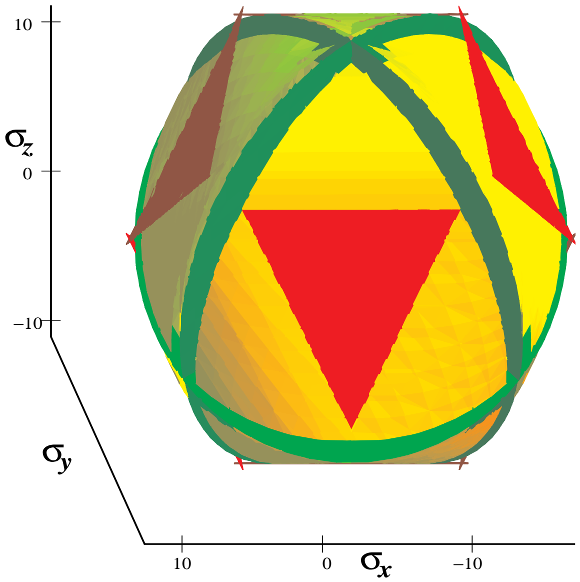

Fig. 4 The black triangular region is the third-rank laminate. White and gray regions show where the second and first-rank laminates are optimal, respectively.

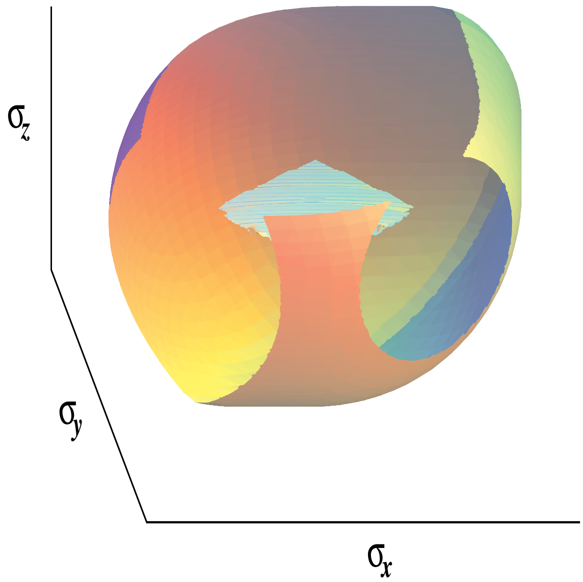

Fig. 6 The interior region of the small ellipsoid defines the bound of the set $\mathfrak{F}_1$, and the region between the ellipsoids defines the forbidden region when one of the materials is void.

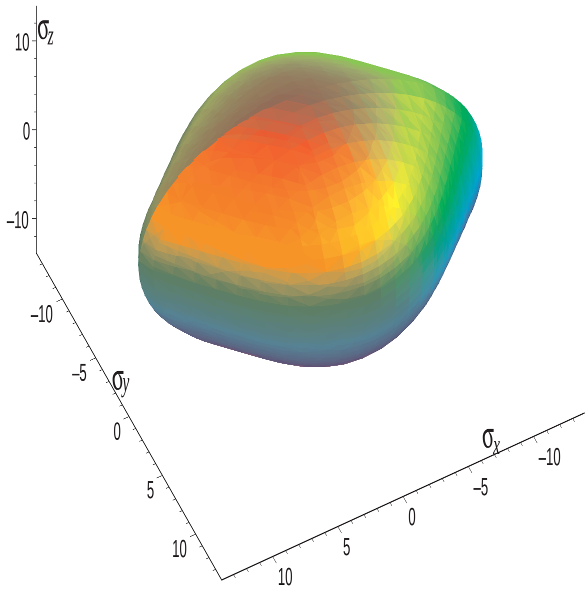

Fig. 5 The intersection of three ellipsoids defines the bound of the set $\mathfrak{F}_2$ when one of the materials is void.

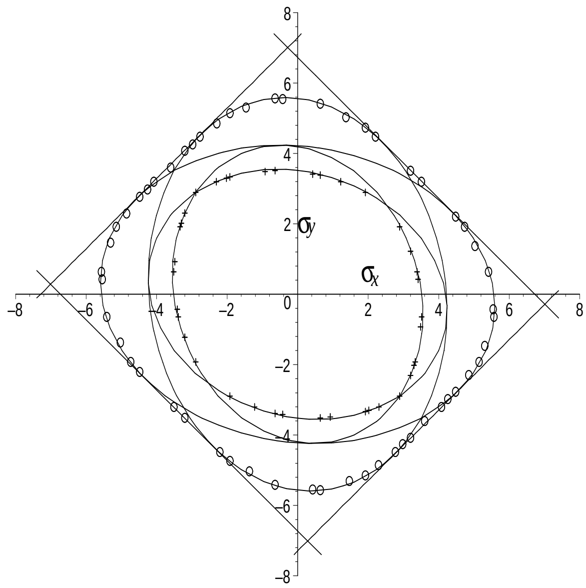

Fig. 7 Two-dimensional case; Region $\mathfrak{F}_1$ lies inside of the region given by crosses, while region $\mathfrak{F}_2$ lies outside of the region given by circles. The forbidden region $\mathfrak{F}_f$ lies between the regions.

The plane component of the boundary of $\mathfrak{F}$ is:

$$\mathbb{E}_3 = D_2(|\sigma_x| + |\sigma_y| + |\sigma_z|)^2| = 1 \qquad (53)$$

where the constant coefficient D_2 is determined by the material constants and it corresponds to stationary values of α and β in (43)−(44). Thus, the boundaries of the forbidden region has three components; the plane, cylindrical and elliptical segments. Note that the components $\mathbb{E}_1 = 1$, $\mathbb{E}_2 = 1$ and $\mathbb{E}_3 = 1$ together define the surface which are a rotationally invariant norm of the stress tensor.

The graph of the permitted fields is presented in Figure 1–Figure 6 for three different pairs of values for elastic moduli; one of the two materials has zero Poisson ratio, both materials have nonzero Poisson ratio and one of the materials is void. Briefly, the weak material is present at the intersection of the three parts mentioned above, and the strong material is observed at the union of three components.

Now we can formulate the underlying principle of stiffness optimization by a two-material structure.

4.2 Optimal Structures

A three-dimensional generalization of the figure obtained for two dimensions in Figure 7 is given in Figure 2, and Figure 4. In Figure 7, we observed Cherkaev and Küçük (2001) that region $\mathfrak{F}_1$ lies inside of the region given by crosses, while region $\mathfrak{F}_2$ lies outside of the region given by circles and the forbidden region $\mathfrak{F}_f$ lies between the regions.

Similarly, the region of $\mathfrak{F}_1$ in three-dimensional case is observed as the inner region of the small ellipsoids in Figure 1, Figure 3 and Figure 6; and the region of $\mathfrak{F}_2$ is observed as the outer part of the ellipsoids in Figure 1, and Figure 5. Consequently, the forbidden region $\mathfrak{F}_f$ appears as a region between the big and small ellipsoids in the figures of Figure 1, Figure 3 and Figure 6.

The optimal structures are not unique in contrast with the regions of optimal fields. It is a known set of optimal geometries that provides the fields inside of them on the boundary of the permitted regions due to adjustment of the inner parameters. These are the same third-rank laminates that we have described earlier.

Suppose that an optimal structure is submerged into a homogeneous external field $\boldsymbol{\sigma}$. If the external field belongs to $\mathfrak{F}_1$ or $\mathfrak{F}_2$, then the optimal design consists of one material $\boldsymbol{\mathcal{S}}_1$ or $\boldsymbol{\mathcal{S}}_2$. The field jumps over the forbidden region along the boundary surface between zones occupied with the strong and weak materials. It turns out that such jumps are possible only if the boundary becomes a curve with infinitely many wiggles, see Cherkaev (2000). As a result, the optimal structure becomes a composite in which the fields belong to the boundaries of $\mathfrak{F}_1 = constant_1$ or $\mathfrak{F}_2 = constant_2$ at each point. To provide this feature, the volume fraction and the inner parameters vary together with the average stress field.

Fields in optimal third-rank laminates If the external field belongs to the pyramid supported by the black triangular regions in the Figure 2, Figure 4, and Figure 8 then the optimal structure corresponds to nondegenerative laminates of the third rank. The directions of laminates are determined by the eigenvectors of the stress $\boldsymbol{\sigma}$. The anisotropy of the structure balances resistance against stresses acting in the orthogonal directions with different magnitudes. The fields in the layers of the first, second, and third rank in the strong (wrapping) materials correspond to three points on the plane triangles shown in black, the field in the first (inner) layer corresponds to the vertex of the triangle, the field in the second layer corresponds to a point on a side of it, and the field in the outer layer corresponds to the point inside the triangle. The corresponding field in the nucleus belongs to the corner of the permitted region (intersection of the three ellipsoids): It satisfies the condition

$$|\boldsymbol{\sigma}_x| = |\boldsymbol{\sigma}_y| = |\boldsymbol{\sigma}_z| = Constant.$$

The corresponding region is shown on Figure 1, Figure 3, and Figure 5.

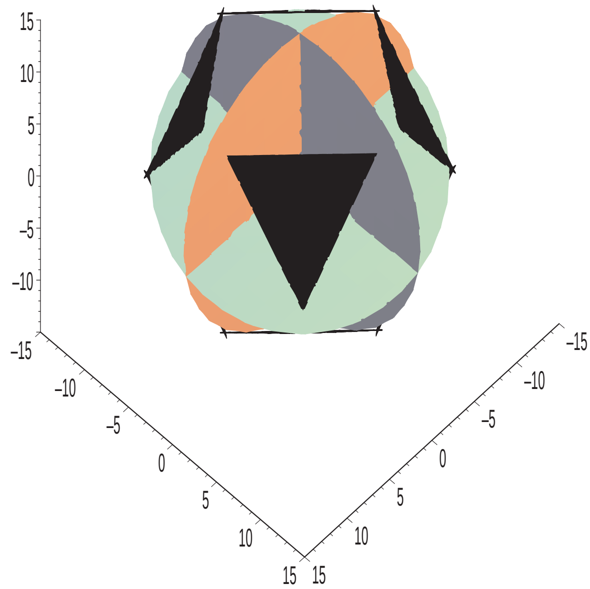

Fig. 8 One of the materials is void. The boundary of the permitted region of the strong material. Observe that the components of the boundary that correspond to optimality of simple laminates disappear.

Fields in optimal second-rank laminates When one of the eigenvalues of the stress tensor is significantly larger than the others, see (46)−(48), the optimal structure degenerates into a second-rank laminate. These regions are shown in white in Figure 2, and Figure 4. The generator of optimal cylindrical inclusions is codirected with maximal eigenstress. Other eigenvectors corresponding to two smaller eigenvalues that determine the normals to the layers in the second-rank laminate. The maximal possible stiffness of this anisotropic structure is codirected with the generator; the optimal structure adjusts itself to equalize the response to stresses of different magnitudes applied in the directions across the generator. The stresses in the wrapping layer correspond to two points along the generator, one of them on the boundary of this domain. they satisfy the relation

$$|\boldsymbol{\sigma}_x| + |\boldsymbol{\sigma}_y| = constant(x) < |\boldsymbol{\sigma}_z|$$

where subindex $_z$ shows the direction of the generator of cylinders. The corresponding stress in the weak material

Fig. 9 Permitted regions in badly-ordered case.

inside the cylinder belongs to the rib of its domain $\mathfrak{F}$; It satisfies the condition

$$|\boldsymbol{\sigma}_x| = |\boldsymbol{\sigma}_y| < |\boldsymbol{\sigma}_z|.$$

Fields in optimal simple laminates The fields in optimal laminate belong to the points of elliptical surface. The fields in both materials are constant, and they correspond to regular points on the elliptical components of the boundaries of the permitted sets.

Badly-ordered case When available materials are badly-ordered, the admissible set of stresses is restricted by elliptic hyperboloids, see Figure 9. The hyperbolic segments of the boundaries replace spherical and cylindrical segments of the boundaries for well-ordered case. In this case, the preferable material is defined not by the intensity of the loading, but by its type: an intensive shear loading requires the material with larger shear modulus, and an intensive bulk loading requires the other material with larger bulk modulus.

4.3 Topology Optimization

The asymptotic case when one of the materials is void is of special interest. The optimal design problem becomes a problem of determining of the shape of the material frame in the design domain, or determining the number and location of holes (voids) in a solid structure. This problem is often called *topology optimization* problem. Our results can be easily reformulated for this case. Here we show the results for the zero Poisson ratio material to keep the notations simple.

Define the norm $\|\boldsymbol{\sigma}\|_T$ of the stress field as following:

$$\|\boldsymbol{\sigma}\|_T = \begin{cases} |\boldsymbol{\sigma}_x| + |\boldsymbol{\sigma}_y| + |\boldsymbol{\sigma}_z| & \text{if } \ |\boldsymbol{\sigma}_x| + |\boldsymbol{\sigma}_y| \le |\boldsymbol{\sigma}_z|, \\ (|\boldsymbol{\sigma}_x| + |\boldsymbol{\sigma}_y|)^2 + |\boldsymbol{\sigma}_z|^2 & \text{if } \ |\boldsymbol{\sigma}_x| + |\boldsymbol{\sigma}_y| > |\boldsymbol{\sigma}_z|. \end{cases} \tag{54}$$

In an optimally designed body, the following conditions are hold inside of the material:

$$\|\boldsymbol{\sigma}\|_T = \begin{cases} > C & \text{if the material is solid,} \\ = C & \text{if the material is involved in} \\ & \qquad\text{an optimal structure.}^1 \end{cases} \tag{55}$$

where C is a positive constraint that depends on the amount of given material and of the intensity of external loading, (see Figure 8).

The formulated result realizes the centuries-old rule of rational design: the material should never be understressed. The material, however, may be overstressed since we cannot do better that place the solid material in the intensively stressed domain.

The optimal structures that realize this requirement are again non-unique, see for discussion in Cherkaev (2000). In particular, the laminate can be used as optimal structures. The first-rank (simple) laminate is never optimal since the structure would break apart in this asymptotical case. The properly adjusted second-rank laminates correspond to cylindrical parts of the surface in Figure 8. The third-rank laminate correspond to plane triangular regions. The volume fraction, orientation, and the geometric parameters of structures vary to make the fields in the material satisfy the conditions (55).

A Terms Used in Section 3.4.1

In this appendix, we give explicit formulas for the terms and an algorithm used in Section 3.4.1. The terms used in (43) and (44) is given as

$$\begin{aligned} \mathfrak{B} \ = \ & 12(-\nu_2^4 + 4\nu_3^3\nu_2 - \nu_3^4 - 6\nu_3^2\nu_2^2 + 4\nu_3\nu_2^3)\mu_h^3 \\ -36 \ & (4\nu_3\nu_2^3 + 4\nu_3^3\nu_2 - \nu_2^4 - 6\nu_3^2\nu_2^2 - \nu_3^4)\kappa_h\mu_h^2 \\ -108 \ & \left(6\nu_3^2\nu_2^2 - (\nu_3^3\nu_2 + \nu_3\nu_2^3) - 2(\nu_2^4 + \nu_3^4)\right)\kappa_h^2\mu_h. \end{aligned} \tag{56}$$

$$\begin{aligned} \mathfrak{N}^{\alpha_1} \ = \ & 2(3\kappa_h\mu_h + \kappa_n\mu_h + 3\kappa_n\kappa_h)\sigma_x - \\ & (\sigma_z + \sigma_y)(6\kappa_h\mu_h - 2\kappa_n\mu_h + 3\kappa_n\kappa_h) \end{aligned} \tag{57}$$

$$\begin{aligned} \mathfrak{N}^{\beta_1} \ = \ & 2(3\kappa_h\mu_h + 3\kappa_n\kappa_h + \kappa_n\mu_h)\sigma_y - \\ & (\sigma_x + \sigma_z)(6\kappa_h\mu_h - 2\kappa_n\mu_h + 3\kappa_n\kappa_h) \end{aligned} \tag{58}$$

$$\mathfrak{D}_1 = \mu_h(-\kappa_h + \kappa_n)(\sigma_y + \sigma_x + \sigma_z) \quad (59)$$

$$\begin{aligned}\mathfrak{N}^{\alpha_2} &= ((-10\kappa_n + 18\kappa_h)\mu_h^2 - 2(\mu_n\kappa_h + 3(\mu_n - \kappa_h)\kappa_n)\mu_h \\ &- 6\mu_n\kappa_h(-2\kappa_h + 3\kappa_n))\sigma_x - ((10\kappa_n - 6\kappa_h)\mu_h^2 \\ &+ (6\mu_n\kappa_n - 10\mu_n\kappa_h + 21\kappa_n\kappa_h - 18\kappa_h^2)\mu_h \\ &- 3\mu_n\kappa_h(-2\kappa_h + 3\kappa_n))(\sigma_y + \sigma_z), \quad (60)\end{aligned}$$

$$\begin{aligned}\mathfrak{N}^{\beta_2} &= ((12\mu_n - 18\mu_h)\kappa_h^2 - (2\mu_n\mu_h - 15\kappa_n\mu_h + 9\mu_n\kappa_n \\ &+ 6\mu_h^2)\kappa_h + 2\kappa_n\mu_h(\mu_h + 3\mu_n))\sigma_x + 2(\mu_h + 3\kappa_h) \\ &\quad (3\kappa_h + \mu_h + 3\mu_n)(\kappa_n - \kappa_h)\sigma_y + (18\kappa_h^3 \\ &+ 6(\mu_n - 3\kappa_n + 2\mu_h)\kappa_h^2 - (9\mu_n\kappa_n + 9\kappa_n\mu_h \\ &+ 10\mu_n\mu_h - 2\mu_h^2)\kappa_h + 2\kappa_n\mu_h(\mu_h + 3\mu_n))\sigma_z, \quad (61)\end{aligned}$$

$$\begin{aligned}\mathfrak{D}_2 &= (-\mu_n + \mu_h)(-\kappa_h + \kappa_n)((6\kappa_h - \mu_h)\sigma_x \\ &\qquad -(\sigma_y + \sigma_z)(3\kappa_h + \mu_h)). \quad (62)\end{aligned}$$

$$\begin{aligned}\mathfrak{N}^{\alpha_3} &= -2(-\kappa_n + \kappa_h)(3\kappa_h + \mu_h)(3\kappa_h + 3\mu_n + \mu_h)\sigma_x + \\ &\quad (18\kappa_h^3 - (18\kappa_n - 6\mu_n - 12\mu_h)\kappa_h^2 + (2\mu_h^2 - 9\kappa_n\mu_h \\ &- 10\mu_h\mu_n - 9\kappa_n\mu_n)\kappa_h 2(3\mu_n + \mu_h)\kappa_n\mu_h)\sigma_y + \\ &\quad ((12\mu_n - 18\mu_h)\kappa_h^2 + (-9\kappa_n\mu_n + 15\kappa_n\mu_h \\ &- 2\mu_h\mu_n - 6\mu_h^2)\kappa_h + 2(3\mu_n + \mu_h)\kappa_n\mu_h)\sigma_z, \quad (63)\end{aligned}$$

$$\begin{aligned}\mathfrak{N}^{\beta_3} &= ((2\kappa_h + 2\kappa_n)\mu_h^2 + (-9\kappa_n\kappa_h + 6\mu_n\kappa_n - 10\mu_n\kappa_h \\ &+ 12\kappa_h^2)\mu_h + 3\kappa_h(-3\mu_n\kappa_n + 2\mu_n\kappa_h - 6\kappa_n\kappa_h \\ &+ 6\kappa_h^2))\sigma_x - 2(\kappa_h - \kappa_n)(3\kappa_h + \mu_h)(3\kappa_h + \mu_h \\ &+ 3\mu_n)\sigma_y + ((12\mu_n - 18\mu_h)\kappa_h^2 + (15\kappa_n\mu_h - 6\mu_h^2 \\ &- 9\mu_n\kappa_n - 2\mu_h\mu_n)\kappa_h + 2(\mu_h + 3\mu_n)\kappa_n\mu_h)\sigma_z, \quad (64)\end{aligned}$$

$$\begin{aligned}\mathfrak{D}_3 &= (\kappa_h - \kappa_n)(\mu_h - \mu_n)((3\kappa_h + \mu_h)(\sigma_x + \sigma_y) \\ &\qquad -(6\kappa_h - \mu_h)\sigma_z) \quad (65)\end{aligned}$$

$$\begin{aligned}\mathfrak{N}^{\alpha_4} &= -2(\kappa_h - \kappa_n)(3\kappa_h + \mu_h)(3\kappa_h + 3\mu_n + \mu_h)\sigma_x \\ &+ ((2\kappa_n - 6\kappa_h)\mu_h^2 + (-2\kappa_h\mu_n - 18\kappa_h^2 + 6\kappa_n\mu_n \\ &+ 15\kappa_n\kappa_h)\mu_h + 3\kappa_h\mu_n(-3\kappa_n + 4\kappa_h))\sigma_y + \\ &\quad ((12\mu_n - 18\mu_h)\kappa_h^2 + (15\kappa_n\mu_h - 6\mu_h^2 - 9\mu_n\kappa_n \\ &- 2\mu_h\mu_n)\kappa_h + 2(\mu_h + 3\mu_n)\kappa_n\mu_h)\sigma_z, \quad (66)\end{aligned}$$

$$\begin{aligned}\mathfrak{N}^{\beta_4} &= ((18\kappa_h - 10\kappa_n)\mu_h^2 + (6\kappa_n\kappa_h - 2\mu_n\kappa_h \\ &- 6\mu_n\kappa_n)\mu_h - 6\mu_n\kappa_h(3\kappa_n - 2\kappa_h))\sigma_y + \\ &\quad ((18\mu_h - 6\mu_n)\kappa_h^2 + (-21\kappa_n\mu_h + 10\mu_n\mu_h + 6\mu_h^2 \\ &+ 9\mu_n\kappa_n)\kappa_h - 2\kappa_n\mu_h(5\mu_h + 3\mu_n))(\sigma_x + \sigma_z), \quad (67)\end{aligned}$$

$$\begin{aligned}\mathfrak{D}_4 &= (\kappa_h - \kappa_n)(\mu_h - \mu_n)((3\kappa_h + \mu_h)(\sigma_x + \sigma_z) \\ &\qquad -(6\kappa_h - \mu_h)\sigma_y). \quad (68)\end{aligned}$$

B
Formulas for Energies

The energy $\mathbb{E}_i^{1R}$ for the first-rank laminate where $\alpha_i = 1$ is defined as follows

$$\begin{aligned}\mathbb{E}_1^{1R} &= \frac{A\sigma_x^2 + B(\sigma_y^2 + \sigma_z^2) - C(\sigma_y + \sigma_z)\sigma_x + D\sigma_y\sigma_z}{18\mu_h^2(4\mu_n + 3\kappa_n)\kappa_h^2} \\ \mathbb{E}_2^{1R} &= \frac{B(\sigma_x^2 + \sigma_z^2) + A\sigma_y^2 - C(\sigma_x + \sigma_z)\sigma_y + D\sigma_x\sigma_z}{18\mu_h^2(4\mu_n + 3\kappa_n)\kappa_h^2} \\ \mathbb{E}_3^{1R} &= \frac{B(\sigma_x^2 + \sigma_y^2) + A\sigma_z^2 - C(\sigma_x + \sigma_y)\sigma_z + D\sigma_x\sigma_y}{18\mu_h^2(4\mu_n + 3\kappa_n)\kappa_h^2}\end{aligned}$$

where

$$\begin{aligned}A &= (9(\mu_h - \mu_n)\kappa_n - 24\mu_h\mu_n + 27\mu_h^2)\kappa_h^2 - \\ &\quad \mu_h(15\kappa_n\mu_h - 4\mu_h\mu_n - 12\kappa_n\mu_n)\kappa_h - 4\mu_n\mu_h^2\kappa_n \\ B &= (-9(\mu_n^2 + \kappa_n\mu_n - \kappa_n\mu_h) + 12\mu_h\mu_n)\kappa_h^2 + \\ &\quad \mu_h(4\mu_h\mu_n + 3\kappa_n\mu_h - 6\kappa_n\mu_n)\kappa_h - 4\mu_n\mu_h^2\kappa_n \\ C &= (3\kappa_h + 4\mu_h)(3\kappa_h\kappa_n\mu_h - 2\mu_h\kappa_h\mu_n - 3\kappa_h\kappa_n\mu_n \\ &\qquad +2\kappa_n\mu_h\mu_n) \\ D &= (18\mu_n^2 - 12\mu_h\mu_n + 9(\mu_n - \mu_h)\kappa_n)\kappa_h^2 + \\ &\quad 2\mu_h(3(\mu_h - 2\mu_n)\kappa_n + 4\mu_h\mu_n)\kappa_h - 8\mu_n\mu_h^2\kappa_n\end{aligned}$$

The energy $\mathbb{E}_i^{3R}$ for the third-rank laminate where all α_i's in (15) are in the interval of $(0, 1)$ is defined as follows

$$
\begin{aligned}
\mathbb{E}_1^{3R} &= \frac{(3\kappa_h + 4\mu_h)(\sigma_y + \sigma_x + \sigma_z)^2(\kappa_h - \kappa_n)}{18\kappa_h^2(3\kappa_n + 4\mu_h)}, \\
\mathbb{E}_2^{3R} &= \frac{AA}{DD}\frac{((3\kappa_h + \mu_h)(\sigma_z + \sigma_y) + (\mu_h - 6\kappa_h)\sigma_x)^2}{18\kappa_h^2\mu_h^2}, \\
\mathbb{E}_3^{3R} &= \frac{AA}{DD}\frac{((-6\kappa_h + \mu_h)\sigma_z + (3\kappa_h + \mu_h)(\sigma_x + \sigma_y))^2}{18\kappa_h^2\mu_h^2}, \\
\mathbb{E}_4^{3R} &= \frac{AA}{DD}\frac{((3\kappa_h + \mu_h)(\sigma_x + \sigma_z) + (\mu_h - 6\kappa_h)\sigma_y)^2}{18\kappa_h^2\mu_h^2},
\end{aligned}
$$

where

$$
\begin{aligned}
DD &= (-36\kappa_h^2 + (36\kappa_n - 24\mu_h - 24\mu_n)\kappa_h \\
&\quad +27\mu_n\kappa_n + 21\kappa_n\mu_h - 4\mu_h^2 + 4\mu_n\mu_h, \\
AA &= (3\kappa_h + 4\mu_h)(\kappa_n - \kappa_h)(\mu_n - \mu_h).
\end{aligned}
$$

C
Algorithm to Find Sets of Fields

In this section, we give an algorithm to obtain sets $\mathfrak{F}_1$ given in (49) and $\mathfrak{F}_2$ given in (50) for each material. Briefly, the optimal energy is calculated through the following algorithm for any given material properties, not necessarily restricted to well-ordered case.

$\mathbb{E} = \mathrm{proc}(\boldsymbol{\sigma}_i, \boldsymbol{\mathcal{S}}_j, \boldsymbol{\mathcal{S}}_i)$

If α_1, α_2 **and** $\alpha_3 \in (0,1)$ $\mathbb{E}_1^{3R}$

Elseif $\alpha_1 = 0$ **then** $\alpha_2 = \alpha_1^{2R1}$ **and** $\alpha_3 = \alpha_2^{2R1}$

If $\alpha_2 \in (0,1)$ **then** $\mathbb{E}_1^{2R1}$

Elseif $\alpha_3 \in (0,1)$ **then** $\mathbb{E}_2^{2R1}$

Elseif $\alpha_2 = 0$ **and** $\alpha_3 = 1$ **then** $\mathbb{E}_3^{1R}$

Elseif $\alpha_2 = 1$ **and** $\alpha_3 = 0$ **then** $\mathbb{E}_2^{1R}$

end

Elseif $\alpha_1 = 1,\quad \alpha_2 = 0$ **and** $\alpha_3 = 0$ **then** $\mathbb{E}_1^{1R}$

Elseif $\alpha_2 = 0$ **then** $\alpha_1 = \alpha_1^{2R2}$ **and** $\alpha_3 = \alpha_2^{2R2}$

If $\alpha_1 \in (0,1)$ **then** $\mathbb{E}_1^{2R2}$

Elseif $\alpha_3 \in (0,1)$ **then** $\mathbb{E}_2^{2R2}$

Elseif $\alpha_1 = 0$ **and** $\alpha_3 = 1$ **then** $\mathbb{E}_3^{1R}$

Elseif $\alpha_1 = 1$ **and** $\alpha_3 = 0$ **then** $\mathbb{E}_1^{1R}$

end

Elseif $\alpha_2 = 1,\quad \alpha_1 = 0$ **and** $\alpha_3 = 0$ **then** $\mathbb{E}_2^{1R}$

Elseif $\alpha_3 = 0$ **then** $\alpha_1 = \alpha_1^{2R3}$ **and** $\alpha_2 = \alpha_2^{2R3}$

If $\alpha_1 \in (0,1)$ **then** $\mathbb{E}_1^{2R3}$

Elseif $\alpha_2 \in (0,1)$ **then** $\mathbb{E}_2^{2R3}$

Elseif $\alpha_1 = 0$ **and** $\alpha_2 = 1$ **then** $\mathbb{E}_2^{1R}$

Elseif $\alpha_1 = 1$ **and** $\alpha_2 = 0$ **then** $\mathbb{E}_1^{1R}$

end

Elseif $\alpha_3 = 1,\quad \alpha_1 = 0$ **and** $\alpha_2 = 0$ **then** $\mathbb{E}_3^{1R}$,
end

The energies used in this algorithm and their notational explanations are given in (69) − (69).

References

Allaire, G., Bonnetier, E., Francfort, G. A., and Jouve, F.: 1997, *Numer. Math.* **76(1)**, 27

Cherkaev, A. V.: 2000, *Variational Methods for Structural Optimization*, Vol. 140, Springer-Verlag, New York; Berlin; Heidelberg

Cherkaev, A. V. and Küçük, I.: 2001, *Structural Optimization*, Submitted

Cherkaev, A. V. and Palais, R.: 1997, *Structural Optimization* **13(1)**, 1

Francfort, G. and Murat, F.: 1986, *Arch. Rat. Mech. Anal.* **94**, 307

Gibiansky, L. V. and Cherkaev, A. V.: 1984, *Design of Composite Plates of Extremal Rigidity*, Report 914, Ioffe Physicotechnical Institute, Acad of Sc, USSR, Leningrad, USSR, English translation in Gibiansky and Cherkaev (1997a)

Gibiansky, L. V. and Cherkaev, A. V.: 1987, *Microstructures of Composites of Extremal Rigidity and Exact Estimates of the Associated Energy Density*, Report 1115, Ioffe Physico-Technical Institute, Acad of Sc, USSR, Leningrad, USSR, English translation in Gibiansky and Cherkaev (1997b)

Gibiansky, L. V. and Cherkaev, A. V.: 1997a, in A. V. Cherkaev and R. V. Kohn (eds.), *Topics in the Mathematical Modelling of Composite Materials*, Vol. 31 of *Progress in nonlinear differential equations and their applications*, pp 95–137, Birkhäuser Boston, Boston, MA, Translation. The original publication in Gibiansky and Cherkaev (1984)

Gibiansky, L. V. and Cherkaev, A. V.: 1997b, in A. V. Cherkaev and R. V. Kohn (eds.), *Topics in the Mathematical Modelling of Composite Materials*, Vol. 31 of *Progress in nonlinear differential equations and their applications*, pp 273–317, Birkhäuser Boston, Boston, MA

Küçük, I.: 2001, *Ph.D. thesis*, University of Utah

Lipton, R. and Diaz, A.: 1995, in N. Olhoff and G. Rozvany (eds.), *Structural and Multidisciplinary Optimization*, pp 161–168, Pergamon, Oxford, UK, 1995, Goslar, Germany

Lurie, K. A.: 1975, *Optimal Control in Problems of Mathematical Physics*, Nauka, Moscow, Russia, in Russian

Lurie, K. A.: 1993, *Applied Optimal Control Theory of Distributed Systems*, Plenum Press, New York ,USA, New York

Olhoff, N., Scheel, J., and Rønholt, E.: 1998, *Structural Optimization* **16**, 1